

**ATTITUDE DETERMINATION AND CONTROL OF
PRATHAM, INDIAN INSTITUTE OF TECHNOLOGY BOMBAY'S
FIRST STUDENT SATELLITE**

**Sanyam S. Mulay,^{*} Jaideep Joshi,[†] Yashovardhan S. Chati,^{*}
Vaibhav V. Unhelkar,^{*} Saptarshi Bandyopadhyay,[‡] Shashank Tamaskar,[§]
Mallesh Bommanahal,^{**} Chaitanya Talnikar,^{††} Avnish Kumar^{*} and
Hari B. Hablani ^{***}**

This paper describes the attitude determination and control sub-system of 'Pratham', a microsatellite being built by the students of Indian Institute of Technology Bombay. Student satellites, such as Pratham, usually have limited sensing, computational and communication capability, motivating the need of autonomous and computationally efficient algorithms. Methods for determining and controlling the attitude with minimal computation load and without any ground support to achieve the desired pointing accuracy are presented. A three axis magnetometer, six 2- π sun sensors and a single frequency GPS receiver are used as the on-board sensors for attitude determination using a single frame method. The attitude controller is designed to achieve an accuracy of 10 degrees in nadir pointing using three orthogonal magnetorquers. Performance of the algorithms is verified through closed loop simulations involving models of the satellite environment, dynamics, actuators and sensors. Lastly, preliminary results of the real time On-board Computer in Loop Simulations are presented.

INTRODUCTION

Students from the Indian Institute of Technology Bombay (IITB) are currently in the process of building a fully functional microsatellite named 'Pratham', which is slated for launch by the Indian Space Research Organization (ISRO), in an 817 km altitude, 10:30 am/pm sun-synchronous orbit. The satellite being built is a 26×26×26 cm cube and weighs nearly 10kg. This landmark student project has completed the phases of Requirements Capture, Conceptual Design, and Preliminary Design and is currently in the Detailed Design Phase. Detailed documentation and thorough reviews have been conducted by ISRO scientists and IITB faculty before the conclusion of each of the above design phases. The goal of the satellite project is to educate

^{*} Undergraduate Student, Department of Aerospace Engineering, IIT Bombay, Mumbai, India.

[†] Research Associate, Centre for Ecological Sciences, IISc Bangalore, Bengaluru, India.

[‡] Graduate Student, Department of Aerospace Engineering, UIUC, USA.

[§] Graduate Student, School of Aeronautics and Astronautics, Purdue University, USA.

^{**} Scientist Fellow, National Aerospace Laboratory, Bengaluru, India.

^{††} Undergraduate Student, Department of Chemical Engineering, IIT Bombay, Mumbai, India.

^{***} Professor, Department of Aerospace Engineering, Indian Institute of Technology Bombay, Mumbai, India

© Pratham, IIT Bombay Student Satellite

students in the field of satellite and space technology in the process of building a satellite to measure the Total Electron Count (TEC) of the Ionosphere.

This paper discusses the Attitude Determination and Control Sub-Subsystem (ADCS) of Pratham. The attitude control requirements on the satellite, imposed by the Payload and Communication Sub Systems, are nadir-pointing accuracy of 10 degrees. The sensors on board the satellite are one single frequency GPS receiver, one three-axis magnetometer and six 2π sun sensors. The Pratham satellite has limited computational capability and does not have an active uplink, hence requiring an autonomous and computationally simple ADCS. With the inclusion of an on-board GPS the attitude determination and control is designed to be autonomous without requiring any ground support. Due to the accuracy requirements and limited computational capability single frame methods are chosen instead of more sophisticated and accurate sequential estimation methods for attitude determination. Attitude determination is carried out using the computationally efficient implementation of the optimal quaternion estimation algorithm (Reference 1) in the sunlit phase of the orbit. In the eclipse phase of the orbit, when no information is available from the sun sensors, no attitude determination and control is carried out.

The control algorithm involves two modes, namely, the detumbling and the nominal mode. The detumbling mode, designed to reduce the high post-launch angular rates of the spacecraft, functions based only on the magnetometer measurements and does not require explicit estimation of the attitude. Once the satellite angular rates are sufficiently reduced, the nominal law controls both the attitude and the rates using the full attitude information. Three orthogonal magnetorquers are used as the actuators. These actuators are designed to provide the required torque using the available power on-board and have been fabricated in-house.

The following figure and Table 1 describe features of the satellite and its orbit, relevant to the attitude determination and control sub-system

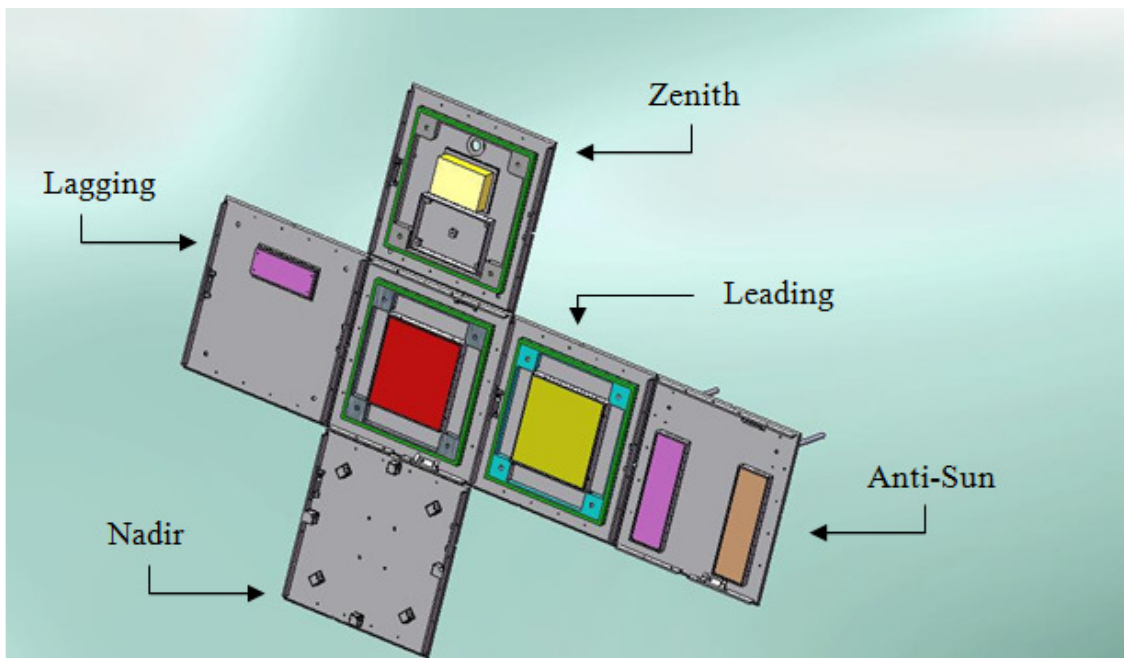


Figure 1. Pratham student satellite (Internal Layout)

We first describe the attitude determination sub-system, which includes details of sensors and attitude determination algorithm. Next, the attitude control algorithms – detumbling mode, nominal mode and the switching condition – are presented. The choice of physical positioning, the error modeling and noise reduction of the sensors are discussed, including some of the design techniques used in reducing on board hardware and software complexity. Performance of the ADCS is first verified through (non-real time) software simulations which include detailed models of the spacecraft environment, dynamics, sensors and actuators. Further, the on-board hardware and software are tested using the On-board Computer In Loop Simulations (OILS). A perfect match is obtained between the real-time OILS and the non-real-time simulations. It is envisaged that this application of simple yet effective attitude determination and control strategies will prove helpful for other student satellite missions all over the world.

Table 1. Satellite Parameters

Characteristics	Value	Unit
Mass	10	kg
Size	26x26x26	cm
Orbit	10:30 Polar Sun Synchronous	-
Altitude	817	km
Orbital period	101	minutes
Moment of Inertia, I	$\begin{bmatrix} 0.116 & -0.0032 & 0.0018 \\ -0.0032 & 0.109 & 0.00014 \\ 0.0018 & 0.00014 & 0.114 \end{bmatrix}$	kg m^2
Desired Attitude Accuracy	Within ± 10	degree
Desired Angular Rate Accuracy	≤ 0.1	$^{\circ}/\text{s}$

Reference Frames

Four reference frames are used in our analysis. The Earth-Centered Inertial (ECI) frame, denoted by subscript ‘I’ has x_I along the vernal equinox, z_I along the celestial north and $y_I = z_I \times x_I$. The Earth Centered Earth Fixed (ECEF) frame is obtained by rotation of the ECI frame about its z axis to maintain the x axis along the intersection of the equator and the Greenwich meridian.^{2,3} The rotating orbit frame has z_o along the nadir, y_o opposite to the satellite’s angular momentum, and $x_o = y_o \times z_o$, and is denoted by the subscript ‘O’. Lastly, the body-fixed frame (subscript: ‘B’) is a frame fixed to the geometric axes of the satellite. In the following sections, vectors are represented in boldface, quaternion in italicized boldface and matrices in majuscules.

ATTITUDE DETERMINATION

The attitude determination sub-system of Pratham employs two types of sensors, namely, a 3-axis Magnetometer and a set of six analog Sun Sensors. Additionally, in order to determine the reference vectors, which are required to compare the measured vectors with, knowledge of the position of the satellite along with pertinent models is required. As the Pratham attitude determi-

nation system was to be designed to be autonomous, i.e. without any ground-aiding, an on-board GPS receiver is used to measure the current position of the spacecraft. In this section, we first describe the selection, characteristics and error models of each of the on-board sensors. Next, we briefly mention the mathematical models for reference vectors, i.e. the model used to determine Earth's magnetic field and the Sun vector. Lastly, we describe how the data from these sensors is combined, in a computationally simplistic manner, to meet the attitude determination accuracy requirement of 10 degrees.

Magnetometer

A three-axis magnetometer is used as one of the primary sensor for the attitude determination of the satellite. The HMR 2300, a magneto resistive digital magnetometer manufactured by Honeywell®, is being used for Pratham, mainly because of its space heritage as well as due to its low weight, size, accuracy and ease of data handling.⁴ Few salient specifications of the magnetometer hardware are tabulated below.

Table 2. Magnetometer Specifications

Characteristics	Value	Unit
Weight	98	g
Size	9.72 x 3.81 x 2.23	cm
Field range	±2	gauss
Field resolution	70	µ gauss
Error (RSS)	0.52	% full scale

The magnetometer measures the magnetic field in body fixed coordinates; these measurements are used directly in the de-tumbling control (B-dot) law, and are processed to obtain the attitude of the satellite once the satellite switches to the nominal mode.⁵ Various sources of error exist in the magnetometer measurements, which need to be accounted for and reduced during design. These errors include additional magnetic field due to on-board electronics and metallic satellite body, mounting errors, errors due to temperature variations, magnetometer drift, bias and random noise. As the magnetometer is surrounded by other satellite electronics, the magnetometer measures along with the earth's magnetic field the field produced due to the satellite body and electronics. In order to reduce the effect of electronics, the magnetometer is optimally placed on the lagging face of the satellite, which is relatively free of all other electronics. Also wire routing is done in such a way that wires carrying currents in the opposite direction are placed together. This prevents formation of magnetic loops and thus stray moment. Other errors are characterized through ground testing of the sensor and are used to model the magnetometer output.

Sensor Model. For modeling and simulation of magnetometer required for the design of ADCS, the above errors are lumped as alignment error (A_{mag}), time-varying (random walk) drift (${}^b\boldsymbol{\epsilon}_{Drift}$), bias (${}^b\boldsymbol{\epsilon}_{Bias}$) and white noise (${}^b\boldsymbol{\epsilon}_{Noise}$). Values and variation in these parameters are obtained by ground testing and calibration of the magnetometer. The above table is indicative of the error values. Measurement equation of the magnetometer, where \mathbf{b} denotes magnetic field, is given as,

$$\mathbf{b}_{meas,B} = A_{mag} T_{BO} \mathbf{b}_{Earth,O} + {}^b\boldsymbol{\epsilon}_{drift} + {}^b\boldsymbol{\epsilon}_{bias} + {}^b\boldsymbol{\epsilon}_{noise} \quad (1)$$

Sun Sensor

Six directional analog solar cells are used as sun sensors, and together determine the sun vector when the satellite is in the sun-lit phase of the orbit. The solar cells are placed on each of the six face centres. The solar cells provide a current output depending on the angle made by the sensor normal with the sun vector based on cosine law,

$$I = I_0 \cos(\theta) \quad (2)$$

where I_0 is the intensity at zero angle. In the eclipse part, the intensity due to all the sources is expected to be close to zero, and hence the sensors don't provide attitude information. Moreover, they are used only in the nominal phase to provide full attitude information with the magnetometer and not during the detumbling phase. Due to the inherent output characteristics of the cells, the field of view of the cells is limited and is less than 180 degrees for each directional solar cell. A simple current to voltage convertor followed by a 10-bit ADC is used to obtain digital values of voltage readings from each SS.

The specific sensors are chosen due to cost and size considerations, and their ability to achieve required accuracy. Positioning of sensors is done by detailed analysis and simulation of the sun sensors so as to maximize the 4π visibility of the sun vector using the available sensors. As each solar cell essentially provides orientation of the sun vector with a known axis, we need at least 3 sun-sensors detecting the sun at a time to correctly determine the sun vector. Construction of the sun vector in body frame using current measurements, is done by selecting the output of the three sun facing solar cells, say \mathbf{c}_i , \mathbf{c}_j and \mathbf{c}_k with corresponding voltage output V_i , V_j and V_k . The three sun facing solar cells are selected based on the relative magnitude of voltage output (the highest correspond to the sun facing cells), while keeping a check to not include antiparallel solar cell. The normalized sun vector in body frame $\hat{\mathbf{s}}_B$ is then given as,

$$\mathbf{c}_m^T \mathbf{s}_B = \cos \theta_m = \frac{V_m}{V_0} = k V_m \quad \text{for } m = i, j, k. \quad (3)$$

Combining the three equations and representing them as a matrix, we have the following expressions, (note that knowledge of V_0 (or k) is not required for calculation of the normalized sun vector in the body frame)

$$\mathbf{C}_m \mathbf{s}_B = k \mathbf{V}_m \quad (4a)$$

$$\mathbf{s}_B = k \mathbf{C}_m^{-1} \mathbf{V}_m \quad (4b)$$

$$\hat{\mathbf{s}}_B = \frac{\mathbf{C}_m^{-1} \mathbf{V}_m}{\left| \mathbf{C}_m^{-1} \mathbf{V}_m \right|} \quad (4c)$$

Sensor Model. A simplistic error model incorporating white noise, saturation and bias is used to model the analog sun sensor current measurements. Quantization error and ADC gain is added further to account for analog to digital conversion. Based on an on-board look up table (obtained from ground characterization) the measured angle for each cell is calculated. In the eclipsed phase of the orbit, the cells provide an output which is of the order of magnitude of the sensor noise.

For both the attitude sensors (magnetometer and sun sensor), the attitude determination algorithm requires information of measured vector as well as reference vector. The reference vectors, which are represented in the orbit frame are determined based on standard models (described in subsection on Satellite Environment Modelling) and knowledge of the current satellite position (which is obtained using the GPS receiver).

GPS Receiver

In contrast with the other two sensors which provide attitude information, the GPS receiver is used for position determination of the satellite. A space grade GPS receiver manufactured by Accord® is used for Pratham. The GPS receiver gives the position and velocity of the satellite in Earth Centered Earth Fixed (ECEF) frame, which are then converted to the Earth Centred Inertial (ECI) coordinates. On-board, due to the high power consumption of the GPS, the GPS receiver is not kept on for the entire time. It is switched on so that the position and velocity readings are obtained every 10 minutes. Intermediate values are propagated using J2 - gravity model. Using the knowledge of current position, transformation from ECI to Orbit frame is derived which in turn is used, along with standard models, to calculate the reference sun vector and magnetic field in orbit frame.

Attitude Determination Algorithm

An efficient single-frame optimal algorithm for quaternion estimation (Reference 1) is used for attitude determination of the sun-lit phase of the satellite orbit. This algorithm reduces to the TRIAD algorithm when very high confidence is placed on information from one sensor as compared to the other. Due to nature of the control law, attitude determination is done only in the nominal mode of flight, i.e. when body angular rates are sufficiently small. When the satellite is in eclipse, due to information from only one sensor, the quaternion cannot be estimated (at least two linearly independent measurements are required to estimate the attitude).

The attitude estimated is given by the quaternion q_{BO} , which represents the orientation of the body frame with respect to the orbit frame. The quaternion estimation algorithm requires two anti parallel reference vectors in the orbit frame and two antiparallel measurement vectors in the body frame. The measurements from the sun sensors (\mathbf{s}_B) and magnetometer (\mathbf{m}_B) provide the measured sun vector and magnetic vector in the body frame. As mentioned above, the on - board models of the sun vector and the geomagnetic field vector are used to provide the reference vectors in the orbit frame (\mathbf{s}_O and \mathbf{m}_O) with the help of position information obtained using the GPS (for details see the section on Simulation). The quaternion estimate is obtained by the following expression,

$$q_{opt} = \begin{cases} \frac{1}{2\sqrt{\gamma(\gamma+\alpha)(1+\mathbf{p}_B \cdot \mathbf{p}_O)}} \begin{bmatrix} (\gamma+\alpha)(\mathbf{p}_B \times \mathbf{p}_O) + \beta(\mathbf{p}_B + \mathbf{p}_O) \\ (\gamma+\alpha)(1+\mathbf{p}_B \cdot \mathbf{p}_O) \end{bmatrix} & \text{for } \alpha \geq 0 \\ \frac{1}{2\sqrt{\gamma(\gamma-\alpha)(1+\mathbf{p}_B \cdot \mathbf{p}_O)}} \begin{bmatrix} \beta(\mathbf{p}_B \times \mathbf{p}_O) + (\gamma-\alpha)(\mathbf{p}_B + \mathbf{p}_O) \\ \beta(1+\mathbf{p}_B \cdot \mathbf{p}_O) \end{bmatrix} & \text{for } \alpha < 0 \end{cases} \quad (5)$$

where,

$$\mathbf{p}_B = \frac{\mathbf{m}_B \times \mathbf{s}_B}{|\mathbf{m}_B \times \mathbf{s}_B|} \quad \mathbf{p}_O = \frac{\mathbf{m}_O \times \mathbf{s}_O}{|\mathbf{m}_O \times \mathbf{s}_O|}, \quad (6a)$$

$$\alpha = (1 + \mathbf{p}_B \cdot \mathbf{p}_O)(a_1 \mathbf{m}_B \cdot \mathbf{m}_O + a_2 \mathbf{s}_B \cdot \mathbf{s}_O) + (\mathbf{p}_B \times \mathbf{p}_O) \cdot (a_1 \mathbf{m}_B \times \mathbf{m}_O + a_2 \mathbf{s}_B \times \mathbf{s}_O) \quad (6b)$$

$$\beta = (\mathbf{p}_B + \mathbf{p}_O) \cdot (a_1 \mathbf{m}_B \times \mathbf{m}_O + a_2 \mathbf{s}_B \times \mathbf{s}_O) \quad (6c)$$

$$\gamma = \sqrt{\alpha^2 + \beta^2} \quad (6d)$$

The constants a_1 and a_2 are to be chosen by the designer based on sensor error covariances, and denote the relative confidence in each measurement. For our attitude determination these constants are chosen as $a_1=0.9$ and $a_2=0.1$.

Angular Velocity Determination

Estimates of angular velocity of the body are required in order to determine the control action during the nominal mode. The expression for angular velocity in terms of quaternion and quaternion rate is given by,

$$\begin{aligned} \boldsymbol{\omega}_{BOB} &= 2 \left(q_0 \mathbf{I}_3 - q_0 [\mathbf{q}_v \times] + \mathbf{q}_v \mathbf{q}_v^T \right) \left(\frac{\dot{\mathbf{q}}_v}{q_0} \right) \\ \mathbf{q} &= \begin{bmatrix} \mathbf{q}_v \\ q_0 \end{bmatrix} \end{aligned} \quad (7)$$

The quaternion rate is obtained using numerical differentiation of quaternion estimates. The estimates obtained thus are prone to have high frequency noise, thus, a digital filter is used to eliminate noise

$$\boldsymbol{\omega}_{k,filtered} = \alpha \boldsymbol{\omega}_k + (1 - \alpha) \boldsymbol{\omega}_{k-1} \quad (8)$$

$$\alpha = \frac{T_{step}}{T_{step} + \tau_w} \quad (9)$$

The choice of the filter parameters is done in a way such that it doesn't interfere with the controller bandwidth. The variable T_{step} denotes the step size (sample period) and is constrained due to the on board computation capability. Moreover, the angular rate estimates are not used just after the eclipse, so as to remove the effect of incorrect estimation of attitude rate (note that no attitude estimate is available in the eclipse phase, which results in incorrect estimate of attitude rate just after eclipse). For our system, T_{step} is taken as 2 seconds and the filter time constant (τ_w) is chosen as 50 seconds.

ATTITUDE CONTROL

The aim of attitude control is to bring the satellite into earth pointing orientation after ejection and to maintain this attitude throughout the period of operation. The control requirements are as follows:

Table 3. Attitude Control Requirements

Sub system	Angle Requirement	Unit
Payload	± 10 (all 3 axis)	degree
Communication	± 10 (nadir side)	degree

Attitude control is required by the communication subsystem to ensure that there is proper signal reception from the satellite. This is not a stringent requirement and can be further relaxed by designing a more complicated ground station. Yaw stabilization requirement is required by the payload. In the first section, we explain the control law employed. Lastly, we explain the actuators used to control the satellite.

Control Law

Different control strategies are employed to stabilize the spacecraft during the detumbling phase and the nominal phase. In the detumbling phase, the objective is to reduce the tumbling of the spacecraft and lower the angular rates below $0.1^\circ/\text{s}$ on all three axes. In this phase B - dot control strategy is employed. This strategy beneficial since it only employs local magnetic field information given by magnetometer to generate the required torque. A low pass filter is employed to reduce the effect of high frequency noise in the magnetometer output. The form of the detumbling controller is given by Equation 10.

$$\mathbf{m}_d = -KB_0 \frac{\dot{\mathbf{B}}_{k,\text{filtered}}}{|\mathbf{B}|} \quad (10)$$

where

\mathbf{m}_d : control magnetic moment

K: gain

$|\mathbf{B}|$: magnitude of Earth's magnetic field

$\dot{\mathbf{B}}_{k,\text{filtered}}$: filtered rate of change of magnetic field

The dynamics of magnetic field rate is obtained by equation 11.

$$\dot{\mathbf{B}}_{k,\text{filtered}} = \beta \omega_k + (1 - \beta) \dot{\mathbf{B}}_{k-1} \quad (11)$$

where

ω_k : angular rate of the spacecraft in the body frame and β is given by Equation 8.

Once the angular rate of spacecraft falls below a particular threshold ($|\mathbf{m}_d| < 0.06 \text{ Am}^2$), GPS can be switched on and state estimation can commence. Once the angular rates have decreased further $|\omega| < |\omega|_{\text{tolerance}}$ and the satellite is in the sunlit phase of the orbit nominal controller is

switched on. These conditions are necessary to ensure the stability of the nominal controller. The form of the nominal controller is given by Reference 5. The form of controller ensures the necessary stiffness and damping in the linear second order dynamics of the spacecraft. Equations 12 - 16 describe the necessary equations for the nominal controller.

$$\mathbf{m}_n = \mathbf{u} \times \mathbf{B} \quad (12)$$

$$\mathbf{u} = K_p \frac{\theta}{|\mathbf{B}|^2} + K_i \frac{\int_{t_0}^t \theta dt}{|\mathbf{B}|^2} + K_d \frac{\omega_{BO}}{|\mathbf{B}|^2} \quad (13)$$

$$\theta = 2\mathbf{q}_v \mathbf{q}_0 \quad (14)$$

$$K_p = I(\omega^2 + 2\delta\zeta^2\omega^2) \quad K_d = I(2 + \delta)\zeta\omega \quad K_i = I\delta\zeta\omega^3 \quad (15)$$

$$\omega = \frac{1}{\zeta T} \quad (16)$$

where \mathbf{m}_n is the control moment, \mathbf{q}_v the quaternion vector part, \mathbf{q}_0 the quaternion scalar part and \mathbf{B} the Earth's magnetic field in body frame of the spacecraft. The values of constants are given in Table 4.

Table 4. Nominal Controller Parameters

Parameter	Value
δ	0.015
T	$0.125 \times T_{orbit}$
ζ	1.15

The following strategy is employed for switching between the detumbling and nominal controllers. For the first 2000 seconds in the orbit, the spacecraft executes the detumbling phase. This ensures that the spacecraft slows down sufficiently for the nominal controller to work. Once the satellite slows down sufficiently ($|\omega| < |\omega|_{tolerance}$) and the satellite is in the sunlight phase, the nominal controller is executed. If anytime during the orbit the angular rates become greater than the threshold, the detumbling controller is executed.

Actuators (Magnetorquers)

Three orthogonal magnetorquers on the faces of the satellite form the actuators. Each torquer is a square coil built in house by winding wires and sticking them onto a square base. The adhesive used is space grade epoxy. The specifications of the torque are tabulated in Table 5 below. It is assumed that all the three torquers are identical. The magnetic field produced by the torque is tested by measuring it with the magnetometer at different points within the coil.

The controller on our satellite requires that the magnetic field generated by the coils has to be both positive and negative. Therefore, the current that has to run through the coils has to be both positive and negative. Since there is only 3.3 V available, the coils will be driven by an H-Bridge in order to make both positive and negative currents flow through the coils. To control the torque provided by the coils, the current flowing through the coils is controlled via Pulse Width Modulation, PWM (which is a well tested method of controlling the current in an inductive circuit). The frequency of the PWM is decided to be 1 kHz.

Table 5. Torquer Specifications

Parameter	Value	Unit
Area	441	cm ²
Resistance	~ 15.6	Ω
Inductance	~ 1	μH
Maximum Moment	0.95	Am ²
Number of Turns	40	-
PWM Resolution	16	bits
Wire Material	Cu	-
Wire Diameter	0.31	mm

SIMULATION

In order to verify the performance of the attitude determination and control sub-system, closed loop simulations using the software MATLAB®-Simulink are developed. The simulations involve the models of true satellite kinematics and dynamics, the space environment, the sensor models, the on - board computations (involving navigation and attitude determination), the control law and the torque actuation.

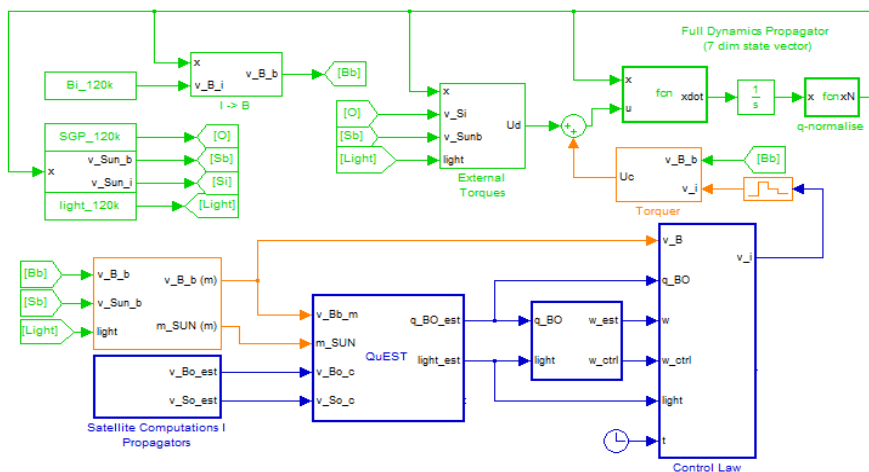


Figure 2. Signal Flow Diagram of Simulations

The signal flow diagram, presented above, includes the spacecraft environment simulation blocks denoted in green. The orange blocks represent the hardware, which include the sensors and actuators. The blue blocks represent the on board computations. The SGP orbit propagator, used to represent the true motion of spacecraft, runs independent of other blocks. It gives the position vector in ECI frame (O). The sun model, which outputs the sun vector (S) in the ECI frame, depends only on time. The geomagnetic field is obtained using the satellite position and the IGRF magnetic model.

Disturbance torques, calculated based on current position and attitude, along with the control torque, are used for propagation of the true attitude dynamics and kinematics, i.e., the true quaternion \mathbf{q}_{BO} and angular rate $\boldsymbol{\omega}_{BOB}$. The hardware blocks along with the true position, rates and attitudes, and using the sensor and actuator models, which include the respective noise characteristics, calculate the sensor outputs. The sun sensor algorithm extracts the sun vector in the body frame (S_B). It also estimates whether the satellite is in the light or eclipse phase. The GPS provides the position and velocity of the satellite at 10 min intervals. The position and velocity are propagated on-board using a simple J2 propagator, fed with initial conditions from the GPS receiver. The position readings are used to calculate the orbit frame magnetic field vector (B_O) and the orbit frame sun vector (S_O) on board using the on board models.

The attitude determination is carried out in the block titled Quaternion Estimation (QuEst), which uses information from sensors and reference vectors to estimate the attitude, and eventually the rate. The estimates of attitude and rate are used to calculate the control torque via the control law. The required torque is then applied by the actuator (magnetorquers). This torque along with the disturbance torques is applied to the real dynamics propagator for state propagation.

This section includes brief explanation of the equations governing satellite dynamics, the models used for simulating the real environment of the satellite and the disturbance torques. The real environment includes the earth's gravity, the sun vector, the geomagnetic field, the regions of eclipse and the disturbance torques.

Satellite dynamics

The dynamics equations involve $\boldsymbol{\omega}_{BIB}$ and \mathbf{q}_{BI} .

$$\dot{\boldsymbol{\omega}}_{BIB} = \mathbf{I}^{-1}(-\boldsymbol{\omega}_{BIB} \times \mathbf{I}\boldsymbol{\omega}_{BIB}) \quad (17)$$

$$\dot{\mathbf{q}}_{BI} = 0.5\Omega \mathbf{q}_{BI} \quad (18)$$

$$\boldsymbol{\Omega} = \begin{bmatrix} 0 & \omega_{BIB}(3) & -\omega_{BIB}(2) & \omega_{BIB}(1) \\ -\omega_{BIB}(3) & 0 & \omega_{BIB}(1) & \omega_{BIB}(2) \\ \omega_{BIB}(2) & -\omega_{BIB}(1) & 0 & \omega_{BIB}(3) \\ -\omega_{BIB}(1) & -\omega_{BIB}(2) & -\omega_{BIB}(3) & 0 \end{bmatrix} \quad (19)$$

Satellite Environment Modeling

Satellite environment modeling aims at simulating the real environment faced by the satellite in orbit. The environment comprises the earth's gravity, the sun vector and the geomagnetic field vector. Since the environment blocks are dependent only on time and are independent of the other blocks in the simulation, they are run offline and the outputs stored. These outputs are then used as environmental inputs to the simulations. This helps in making the simulations faster. The environment variables are generated at small time steps of 0.1 s. These time steps are smaller than those at which the onboard calculations run.

Real Orbit Propagator. The real orbit propagator assumed is the SGP (Simplified General Perturbations) model. This is the simplest orbit propagator for orbits with periods < 225 minutes. It iteratively captures the earth's gravity at any point in the satellite's orbit by including effects of J2 (primary to the existence of sun synchronous orbits), J3, secular and periodic effects of gravitation and the short term perturbations and eliminated where possible. The inputs to the SGP model are the Two Line Elements (TLE) generated by NORAD at epoch and the time. The output of the model is the position vector and the velocity vector of the satellite [O] in the ECI frame.

Sun Model. The sun model is used to get the sun vector in the ECI frame [Si]. The sun vector is also obtained in the body frame [Sb] by a simple transformation from the ECI to the body frame. The input to the model is the time elapsed since the latest vernal equinox. Simple spherical trigonometric relations are used to calculate the sun vector.

Magnetic Model. The International Geomagnetic Reference Field 2011 (IGRF - 11) order 13 model is used to get the geomagnetic field at the satellite's location in its orbit. The input to the model is the position vector of the satellite in the ECI frame. The output is the geomagnetic field vector in the ECI frame [Bi]. The geomagnetic field vector is also obtained in the body frame [Bb] by a simple transformation from the ECI to the body frame.

Light Model. The light model is used to identify whether the satellite is in eclipse phase or not. The satellite is assumed to be a point mass. The sun and the earth are assumed to be finite size spheres. When in the umbra or penumbra of the earth, the satellite is in the eclipse phase and the sun sensors give no readings. The input to the light model is the position vector of the satellite in the ECI frame. The output is a Boolean number ([Light]). If the Boolean value is 1, the satellite is in light. Otherwise, the satellite is in eclipse.

We now describe the disturbance torques which include the gravity gradient torque, the solar drag torque and the aerodynamic drag torque. All the three torques are added to give the net disturbance torque in the body frame about the satellite center of mass. The modeling equations are given below.

Gravity Gradient Torque. The gravity gradient torque is given by

$$\tau_{GG} = \frac{3\mu}{|\mathbf{r}_B|^5} \mathbf{r}_B \times I \mathbf{r}_B \quad (20)$$

where, μ : gravitational parameter for the earth, \mathbf{r}_B : position vector of the satellite in body frame, I : inertia matrix of the satellite.

Solar Drag Torque and Aerodynamic Drag Torque. Solar radiation exerts a drag force on the satellite and hence, a corresponding torque. The force is given by

$$\mathbf{F}_{solar} = -A_p C_a P_{flux} \hat{\mathbf{v}}_{SB} \times \mathbf{light} \quad (21)$$

where, A_p : projected area of the satellite, C_a : drag coefficient, P_{flux} : solar flux on the satellite, and $\hat{\mathbf{v}}_{SB}$ unit sun vector in the body frame. The atmosphere also exerts a drag force (and hence a corresponding torque) on the satellite. This force is given as,

$$\mathbf{F}_{aero} = -0.5 A_p C_D \rho |\mathbf{v}_B|^2 \hat{\mathbf{v}}_B \quad (22)$$

where, C_D : drag coefficient, ρ : atmospheric density, \mathbf{v}_B : position vector of the satellite in body frame. The torques (about the center of mass) is given by the forces crossed with the vector from the satellite center of mass to the satellite center of pressure (where the forces are assumed to act).

SIMULATION RESULTS

This section describes the results of software simulations explained earlier. Multiple simulations were carried out in a Monte Carlo-based scheme, by varying the post-launch initial conditions of attitude and angular rates. Here, we present results of a representative simulation run, for which the initial conditions were taken as,

Table 6. Initial Conditions

Characteristics	Value	Unit
Attitude (with respect to Orbit Frame)	$[+10 \ -32 \ +88]^T$	degree
Angular Rate (ω_{BOB})	$[+1 \ +0 \ -0.5]^T$	/s

Measurement

The attitude sensors, magnetometer and sun sensor, give the information of magnetic field vector and sun vector along with some noise. In order to observe, how accurately the sensors provide measurements we observe the time history of measured (obtained from sensor models) and true (obtained from standard reference models) vectors. The x axis represents the time since launch, mentioned in terms of number of orbits traversed since launch. The eclipse phase of each orbit is denoted by grey background, to emphasize the difference in attitude determination and control strategies in the sun-lit and eclipse phase.

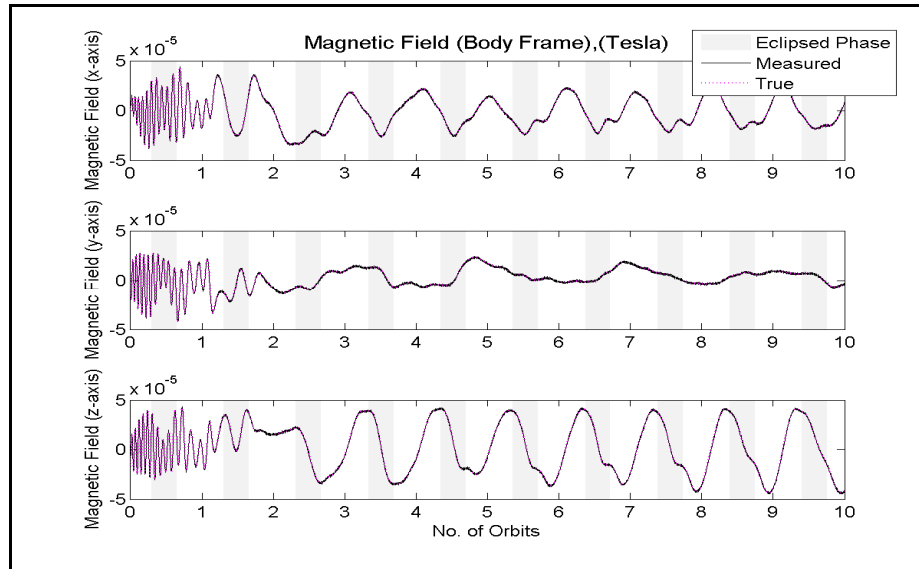


Figure 3. Magnetometer Measurements

The following figure represents the sun vector measurements constructed based on the measurements from the six solar cells. Note that no sun vector measurements are available in the eclipsed phase of the satellite,

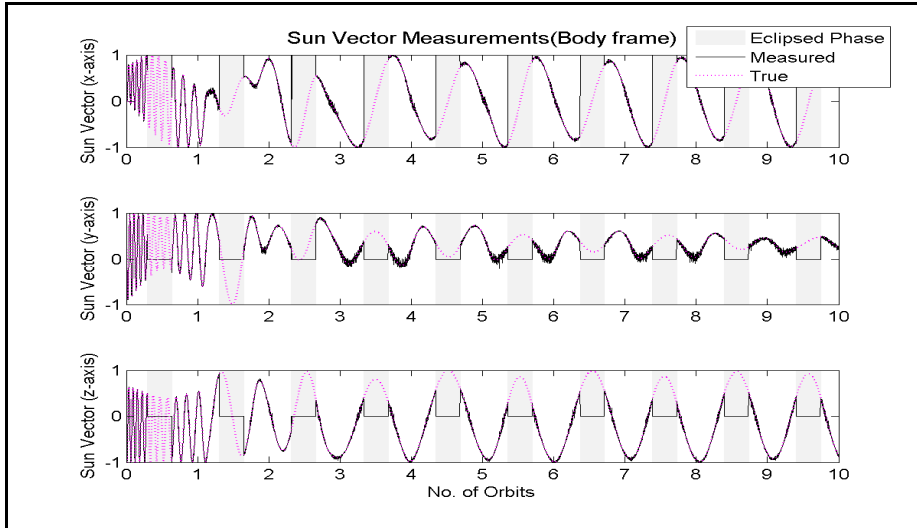


Figure 4. Sun Vector Measurements

Determination

Quaternion estimates using the optimal deterministic method described earlier are presented. To reiterate, no information of attitude is available in the eclipse phase,

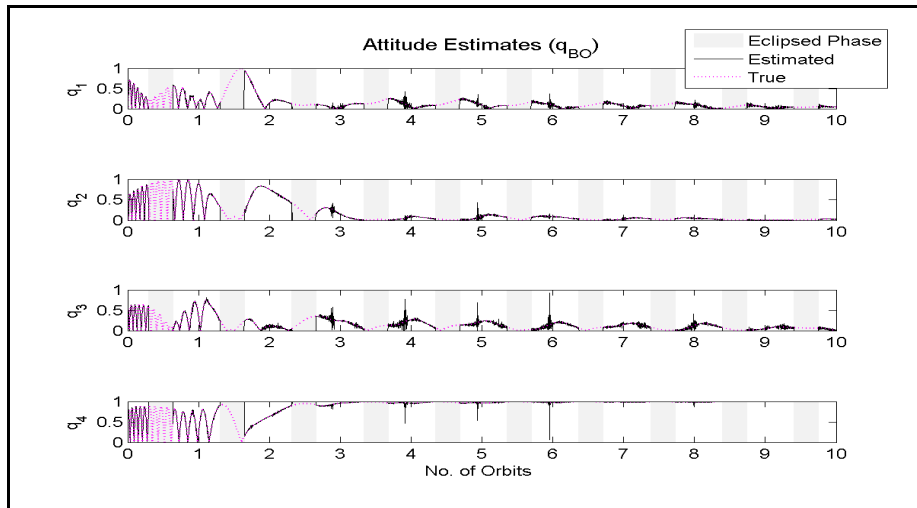


Figure 5. Attitude Determination

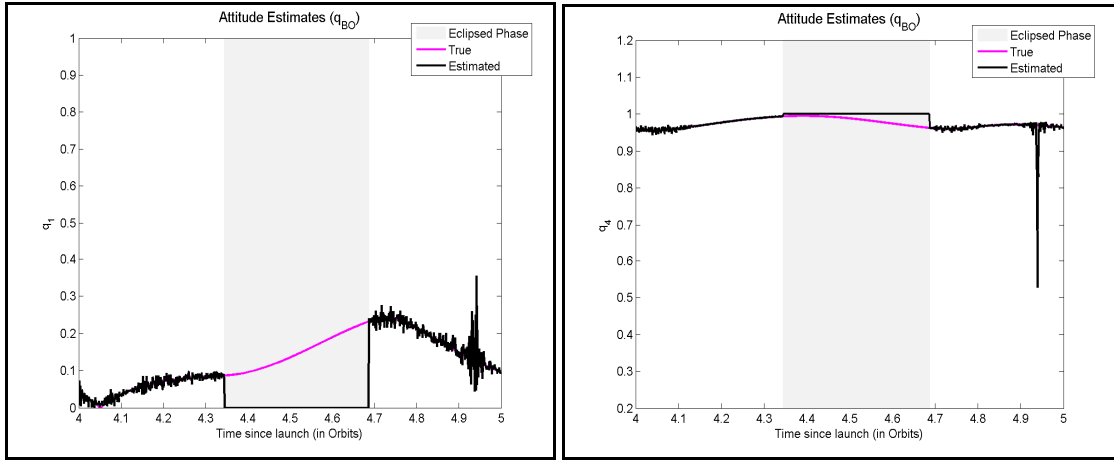


Figure 6. Attitude Determination II

The rate of change of the quaternion along with the low pass filter, provides the information of the angular velocity. Due to the inherent noise of sensors and the error introduced due to numerical differentiation, the errors in both the attitude estimates (as seen in the figure above) and the estimates of angular rates are substantial.

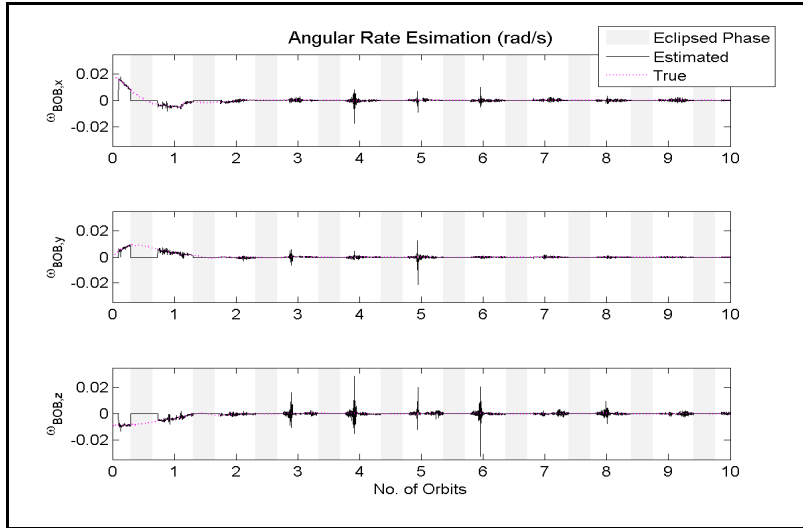


Figure 7. Angular Rate Estimates

Control

Based on the attitude determination, the desired rate and attitude, and the control law the required control torque is calculated. As expected, the requirement of control torque is higher in the detumbling mode, as compared to the nominal expected. Once the satellite enters the nominal

control mode no control torque is applied in the eclipse phase (note that since detumbling control law does not require sun sensor measurements, control is unaffected by the eclipse phase). Although due to limitations of available current and size of the torque the maximum control torque that can be applied is limited, we observe that the magnetorquers are never saturated, i.e., the required torque is well within the saturation limits. Lastly, total power required for control action and the available power on-board the satellite is compared, and it is observed that the power consumption required for ADCS is less than that accounted for by the power budget of the satellite.

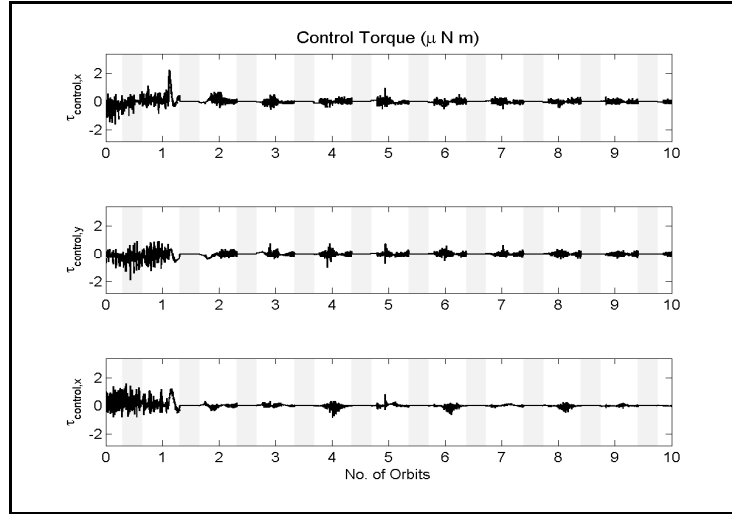


Figure 8. Applied Control Torque

The following results show the controlled attitude and angular rate of the spacecraft. It takes, on an average, around three to four orbits for the attitudes and rates to converge,

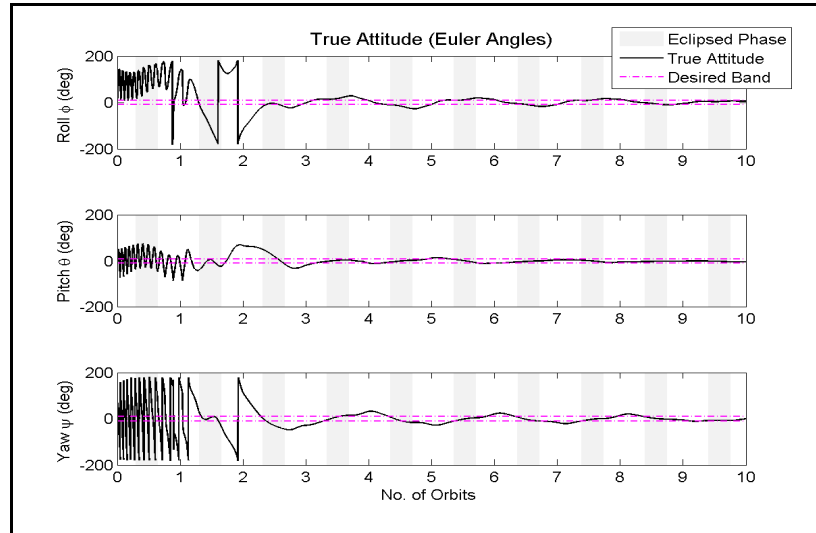


Figure 9. True Attitude (Euler Angles)

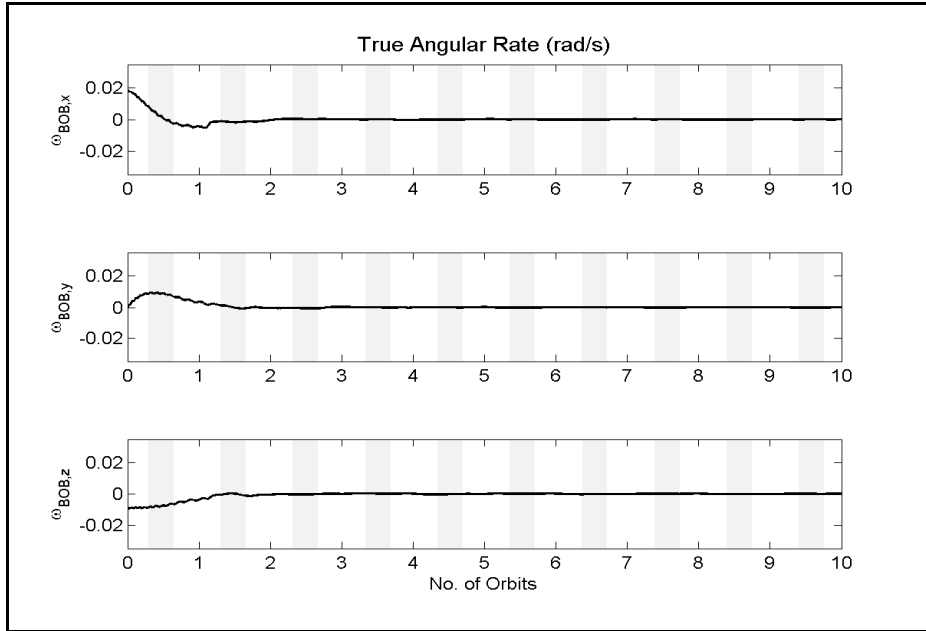


Figure 10. Angular Rate

Although here we show the results from only one simulation run, similar trends were observed for the Monte Carlo - based simulations performed for our system. Next, we discuss the real time On-board Computer in Loop Simulations.

ON-BOARD COMPUTER IN LOOP SIMULATION

The on-board hardware and software are tested using the OILS setup. The setup was made using x-PC Target block set in Simulink. This block-set is used to have the environment model in Simulink simulation interact with flight hardware in real time. NI-PCI-6229 and NI-PCI-6703 data acquisition cards by National Instruments®, were used for hardware interfacing with the target-PC. As described above, the entire simulation can be compartmentalized into three major blocks - the Environment Block, The Attitude Determination and Control Block and the Dynamics Block. The Attitude Determination and Control Block is replaced by the flight hardware, the overall structure of the simulation remains the same. Input to flight hardware - The Environment Block - is the source of sensor input to the flight hardware. The sensor data is computed based on the current position and attitude of the satellite. GPS data is sent every second and the magnetometer data is sent when polled, on the two Universal Asynchronous Receiver/Transmitter (UART) channels of the flight hardware. The sun sensor data is input to the flight hardware in the form of voltages on six Digital to Analog Converter (DAC) channels of the NI-PCI-6703. Outputs from the flight hardware, the response of the On-board Computer, are in the form of a 1 kHz Pulse Width Modulation (PWM), for driving the torquer coils. The PWM is passed through a passive low pass filter and is then recorded at 100 Hz by the analog to digital converter (ADC) of the NI-PCI-6229. The voltages are then converted to currents in the respective coils, consequently to moments in body frame and are then fed to the Dynamics Block, which in turn generates the new state of the satellite, hence completing the loop.

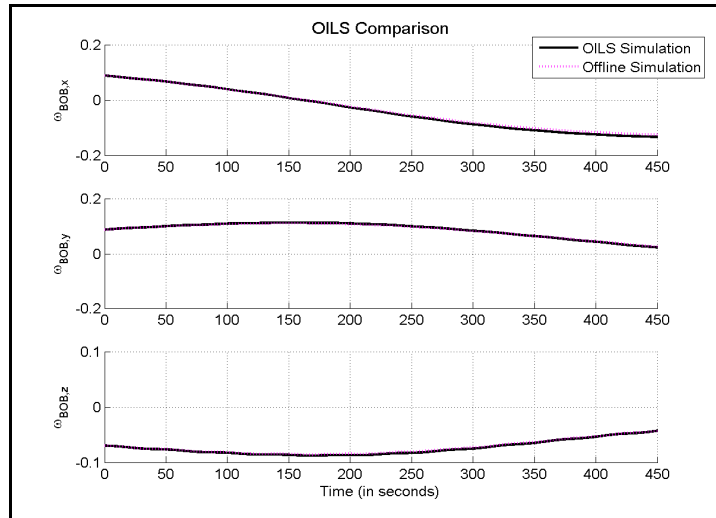


Figure 11. Comparison of OILS with Offline Simulations

CONCLUSION AND COMMENTS

The results of the simulations successfully demonstrate the use of a simple controller and control structure to achieve moderate pointing accuracies and a very good rate control, facilitating its use by student satellites. The autonomy, in terms of no requirement for uplink, provided by the controller simplifies ground operations. The very good match between the real-time simulations with flight hardware in-loop with non-real-time simulations validates the methodology.

ACKNOWLEDGMENTS

We would like to thank the entire team of the Pratham student satellite. Special thanks are due to all the Faculty Mentors of this project, and specifically to Prof. K. Sudhakar, Prof. H. Arya, and Prof. P.M. Mujumdar of the department of Aerospace Engineering, IIT Bombay, who have been a constant source of inspiration and knowledge. Lastly, we would like to acknowledge the excellent support, both technical and financial, that we received from various departments of Indian Space Research Organization and Indian Institute of Technology Bombay.

REFERENCES

- ¹ F. L. Markley, "Fast Quaternion Attitude Estimation from Two Vector Measurements", *Journal of Guidance, Control and Dynamics*, Vol. 25, No. 2, 2002, pp. 411 – 414.
- ² J.R. Wertz, ed., "Spacecraft Attitude Determination and Control", *Dordrecht, Holland, D. Reidel*, 1978.
- ³ M.J. Sidi, "Spacecraft Dynamics and Control: A Practical Engineering Approach", *Cambridge University Press*, 2000.
- ⁴ Honeywell® HMR 2300 magnetometer datasheet
- ⁵ F. Martel, P.K. Pal, M.L. Psiaki, "Active Magnetic Control System for Gravity Gradient Stabilized Spacecraft", *Proc. 2nd Annual AIAA/USU Conf. on Small Satellites*, Sept. 1988, Logan, Utah, pp. unnumbered.

⁶ D.Y. Hsu, “Comparison of 4 Gravity Models”, *Position Location and Navigation Symposium 1996, IEEE 1996*

⁷ C.C. Finlay et al., “International Geomagnetic Reference Field: the eleventh generation”, *Geophys. J. Int.*, Vol. 183, Issue 3, 2010, pp. 1216 – 1230.

⁸ F.R. Hoots, R.L. Roehrich, “Models for Propagation of NORAD Element Sets”, *Spacetrack Report No. 3*, 1980

⁹ F. Markley, “Spacecraft Attitude Determination Methods”, *Israel Annual Conference on Aerospace Sciences, 2000*

¹⁰ “Pratham IIT Bombay Student Satellite – Critical Design Report – Attitude Determination and Control System (ADCS) for Pratham”, 2010

¹¹ Laboratory for Electro – Optic Systems, Indian Space Research Organization sun sensors datasheet